# Microfluidic Pressure in Paper (μPiP)

Md. Nazibul Islam[1], Zachary R. Gagnon[1]*

[1]Artie McFerrin Department of Chemical Engineering, Texas A&M University

*Corresponding author: zgagnon@tamu.edu

## Abstract

We present a simple, low-cost and scalable method for fabricating externally pressurized paper-based microfluidic devices. Known as microfluidic pressure in paper (μPiP), devices fabricated by this technique are capable of sustaining a pressure gradient for use in precise liquid handling and manipulation applications. In addition, the simple nature of this fabrication technique allows device designs to be scalably manufactured and deployed with minimal time, equipment and training requirements. This new platform democratizes the field of microfluidics and offers budget-friendly technology for both academic device prototyping and largescale commercial device production.

Microfluidic engineering and microfabrication technology go hand-in-hand. Historically, advancement in microfluidic capabilities have been synergistically linked to novel advancements in microfabrication technology. In the last two decades, for example, there has been an explosion of new microfluidic systems and devices made technologically feasible largely in part by the invention of soft lithography. Today, soft lithography microfluidics receives significant attention from both academia and industry, and researchers report thousands of new prototype devices each year for use in a broad range of environmental, pharmaceutical and biomedical engineering applications [1-3]. While the global microfluidics market size is expected to reach USD $31.6 billion by 2027 [4], very few of these microfluidic devices are successfully translated to commercial products [3]. One reason for low market penetration is the absence of low-cost high throughput manufacturing technique that can bridge the gap between budget-friendly academic prototyping efforts and often high budget commercial scalability requirements conventionally satisfied by modern industrial manufacturing techniques [1-3, 5]. In academia, soft lithography has been a predominant choice for the fabrication of microfluidic devices [1, 3, 5]. While effective in prototyping, this method is labor-intensive, requires a cleanroom facility and is not easily scalable. In contrast, in a commercial

setting the largescale manufacturing of microfluidic devices is typically accomplished using injection molding or hot embossing techniques [1, 5]. These methods have significantly higher throughput and are capable of manufacturing thousands of devices per day. However, such manufacturing techniques often require large upfront capital equipment, tooling and development costs. While powerful and mature, these fabrication methods are often financially infeasible for an academic or small commercial start-up interested in commercializing their work and can serve as both financial and technical barriers to translation of microfluidic technology from a single prototype device to the commercial marketplace.

Over the past decade, paper-based microfluidics has gained widespread attention as a novel method for creating microfluidic devices for use in low-resource settings [6-9]. Paper is hydrophilic in nature and different techniques such as, photolithography, plasma oxidation, cutting, and wax printing can be used to create and pattern hydrophobic zones within a paper matrix to create no-flux liquid boundaries and direct microfluidic flows. Fluid transport typically takes place passively within the porous paper structure via capillary action [7, 10, 11], and paper-based microfluidics has been used extensively for lateral flow assays and colorimetric detection devices [6, 8, 12-15]. However, a lack of active fluid control and variability in fluid transport due to evaporation is a major limitation for paper-based microfluidic devices [8]. Such a lack in reproducibility and controllability in real-world environmental conditions have limited paper-based microfluidics from successfully competing with PDMS and injection molded technologies [6, 9].

In this work, we report a novel low-cost microfluidic method for rapidly manufacturing and operating laminated paper-based microfluidic devices. We call this method “Microfluidic Pressure in Paper” (µPiP). The laminated nature of this approach enables the paper channels to support an external pressure to control the on-PIP fluid flow in a manner similar to that of conventional microfluidic channels. The µPiP fabrication workflow is depicted in Fig. 1. The entire fabrication process, from design to µPiP device, takes less than 10 minutes. The fabrication begins by first cutting a microfluidic channel geometry from a sheet of filter paper (Whatman Grade 1) using a $CO_2$ laser cutter (PLS6.120D, Universal Laser System, Inc.). The laser can precisely and rapidly cut

hundreds of paper channels with a dimension as small as 100 µm across large area (~1 $m^2$) sheets of paper. Each paper channel is then sealed between two thin flexible sheets of polydimethylsiloxane (PDMS). Depending on the desired stiffness of the µPiP device, sheets of different thickness can be used. For work presented here, channels were laminated between a 0.5 mm PDMS sheet (0.02 inch, McMaster-Carr) as a “top” layer and a 0.12 mm PDMS sheet (0.005 inch, McMaster-Carr) as the “bottom” layer. Fluidic channel inlets/outlets were hole punched on the top PDMS sheet using a biopsy punch (Ted Pella, Inc). The two sheets were then oxidized and irreversibly bonded together using oxygen plasma generated with a handheld tesla coil (Electro-Technic Products, Model BD-20AC). Lastly, the sealed PDMS device was immediately placed into a small 3-Ton manual heat press (Dulytek DW 400) at a temperature of 95$^o$C for 5 minutes which removed all observable air gaps and bubbles surrounding the paper channel structure. Tubing was then inserted into the fluidic inlet and outlet ports on the top of the PDMS sheet and a low-cost constant pressure system (fabrication cost ~USD $500) [16] was used to drive flow fluid through the paper channels. The resulting µPiP devices are flexible, tightly laminated, and capable of sustaining continuous pressure driven flows (Fig. 2). Pressure driven fluid flow through the resulting µPiP channels can be controlled in a manner similar to that of conventional microfluidic devices, in that a fluid flow can be actively regulated through the modulation of an applied external pressure to a fluidic channel inlet or outlet port. Although laminated paper-fluidic devices using various techniques have been reported previously [17, 18], to the best of our knowledge this is the first time an external flow system has been used to drive pressure driven flow through paper-based microfluidic channels.

We now present experiments demonstrating the flow behavior of µPiP channels using external pressure, and how this differs from conventional non-laminated paper-based devices. In non-laminated paper-based devices fluid flow occurs passively via capillary action, and the Lucas-Washburn equation has been successfully used to model flow through paper by this mechanism [19, 20]. The majority of these paper-based devices are open to the external environment, and flow can therefore be influenced by liquid evaporation. While the Lucas-Washburn equation model does not consider this transport

contribution, Liu *et al.* modified this expression to include an evaporative contribution when predicting the fluid wicking length ($h_{ev}$) through a paper channel [19]:

$$h_{ev} = 2N \cdot e^{-Mt} \int_0^{\sqrt{t}} e^{Mt^2} dt \qquad (1),$$

$$\text{where, } N = \sqrt{\frac{\sigma \cos(\theta)}{\mu} \frac{K}{\epsilon R}} \text{ and } M = \frac{2m^*_{ev}}{\rho \varepsilon \delta}$$

Here, N is a modified version of Lucas-Washburn equation based on a momentum balance between capillary pressure and viscous stress. Here, $h_o$, $\sigma, \theta, \mu, K, \epsilon, R$, and $t$ are the theoretical wicking liquid front height, interfacial tension, viscosity, contact angle, permeability, effective pore size, paper pore radius, and time, respectively. The second term, M indicates total evaporation mass. Here, $m^*_{ev}$, $\rho$ *and* $\delta$ are evaporation rate, density and paper strip thickness respectively. This term is used in Eq. 1 to determine the effect of evaporation on wicking height over a time period of t. Because paper channels in µPiP are enclosed in two PDMS membranes, fluid transport by evaporation through PDMS was calculated to be only 1.03% of the rate of evaporation at experimental laboratory conditions (25$^o$C, 35% Relative Humidity). Therefore, we neglected the influence of evaporation and fluid flow in a pressurized µPiP channel was assumed to be driven through a linear combination of capillary wetting and transport in a porous media by a pressure gradient. Combining Darcy's Law with the Lucas-Washburn equation, and neglecting evaporation, the theoretical µPiP liquid penetration height ($h_o$) as a function of time, $t$ is:

$$h_o = \sqrt{\frac{4\sigma \cos(\theta)}{\mu} \frac{K}{\epsilon R}} \cdot t^{1/2} + \frac{K \Delta P}{\mu L} \cdot t \qquad (2),$$

where the first term in Eq. (2) captures the influence of capillary wetting and the second is the contribution to flow via an applied pressure gradient ($\Delta P$) over a channel length, $L$ for a given time, $t$. To evaluate the proposed model with experimental data, available physical parameters of water and Whatman #1 filter paper were used (interfacial tension: 727.1X10$^{-4}$ N/m, contact angle: 80$^o$, viscosity: 9.6075X10$^{-4}$ Pa.sec, density: 997.05 kg/m$^3$, paper thickness: 0.18 mm and, mean fiber radius: 0.0082). Permeability of paper, $K$ for a given pore size, $r$, was calculated using Eq. 3 [19]:

$$K = r^2 \frac{\pi\varepsilon(1-\sqrt{1-\varepsilon})^2}{24(1-\varepsilon)^{1.5}} \qquad (3),$$

Wicking height was tracked in µPiP channels fabricated from Whatman #1 filter laser cut into strips 2 mm in width and 100 mm in length (Fig. 3). The liquid penetration height for a given pressure drop was measured and then compared to the conventional passively driven non-laminated microfluidic equivalent. Flow was characterized using deionized water labelled with 5% w/v methylene blue (Sigma Alrich). Shown in Fig. 3a, under the application of a continuous and fixed externally applied pressure, liquid transport was observed as a moving liquid front advancing down the length of the paper channel. The resulting length of this front was then dynamically measured for different inlet pressures: 0.0 psi (e.g. pure capillary wetting), 0.5 psig, and 1.0 psig. During the flow experiments, high-resolution images were captured every 30 seconds for a period of 300 seconds using a high resolution DSLR camera (Fig. 3b). For pure capillary flow in an open channel (i.e. non-laminated), the effective porosity was calculated using Eq. (1) and determined to be $\epsilon = 0.65$, which is in agreement with previously published data for Whatman #1 filter paper [19, 21]. The paper channels were then encapsulated in PDMS sheets according to the µPiP fabrication workflow and the fluid flow experiment was repeated at a pressure of 0.0 psig. As shown in Fig. 3c, the rate of the moving front in encapsulated channels is reduced approximately 62% when compared to open channels. From Eq. (1), the effective porosity of the laminated µPiP channel was calculated to be 0.25. Therefore, we speculate that the heat press and subsequent hydraulic encapsulation of the paper channels in PDMS sheets likely results in a decreased effective porosity of paper channels and results in a decreased flow.

We next investigated the influence of a pressure gradient on the liquid wetting length for two different non-zero inlet pressures: 0.5 psig and 1.0 psig, and an outlet pressure vented to atmosphere (0.0 psig). As shown in Fig. 3b, there is an observed increase rate of wicking height with applied pressure. Further, unlike the two purely capillary flow experiments in which the observed liquid velocity decreases with increasing transport time, the pressurized fluid velocity (wicking height length per unit time) remains approximately constant (constant slope) with transport time over the period of 300 seconds.

The ability to drive a continuous flow in µPiP channels using external pressure can be exploited to drive a continuous flow in more complex fluidic channel geometries, and for precise control of their subsequent liquid handling. We therefore sought to use µPiP to fabricate and demonstrate pressure-driven flows in other common microfluidic channel geometries constructed from paper. For each device, the fluidic flow field was imaged using deionized water labelled with colored dye, driven continuously into each device at an external pressure of 1.0 psig. We first created the classic Whiteside's microfluidic "Christmas tree" gradient generator (Fig. 4a). To the best of our knowledge at the time of writing, this is the first reported case of a constant concentration gradient produced using continuous flow on a paper device. This functionality suggests µPiP can be utilized as a simple and low-cost alternative to complex microfluidic devices for chemotaxis and pharmaceutical drug performance analysis. Microfluidic pressure in paper (µPiP) was also used to fabricate and successfully drive other common microfluidic channel geometries, including serpentine mixers (Fig. 4b), Y-channels (Fig. 4c), and H-filters (Fig. 4d).

µPiP can also be used with more complex biofluids such as blood (Fig. 5a) and crude oil (Fig. 5b). For these flow experiments we used µPiP fabrication with larger pore glass paper (Ahlstrom-Munksjo grade 1667 lateral flow paper), which is designed for blood plasma separation as it possesses a large 30 µm pore size to allow red blood cells to flow [22]. A suspension of bovine red blood cells (10% v/v in PBS solution, Quad Five) was driven through this paper channel for 10 min at an inlet pressure of 1.0 psi. Crude oil was also successfully driven through the paper with this style of channel, further demonstrating the potential versatility and robustness of this simple pressurized paper platform.

µPiP can also be used with water soluble paper to fabricate open-ended PDMS microchannels without soft lithography. In this technique we used a sheet of water-soluble paper (SmartSolve Industries) as a sacrificial µPiP channel (Fig. 5c). After lamination in PDMS, the paper was washed from the laminated area leaving an open-ended channel in the shape of the laser cut paper geometry. This technique can be used to fabricate PDMS-style fluidic channels in millimeter range without a cleanroom.

In conclusion, we have demonstrated a microfluidic fabrication technique for producing laminated paper microchannels. Devices fabricated using the µPiP technique can be controllably pressurized for use in active fluid flow control. A mathematical transport model based on capillary and pressure driven flow was developed and shown to accurately describe the µPiP flow behavior. A variety of microfluidic designs and complex fluids can be utilized using this method, and the fabrication workflow will enable researchers to quickly design, build, test, and share device designs with minimal effort. Further, because small portable laser cutters and tesla coils can be used for device fabrication, it is feasible to design µPiP devices at a central location then share, fabricate and deploy these devices “on-demand” in distant remote areas such as war zones, outer space or in rural low-resource settings. This fabrication technique is also scalable - the µPiP fabrication workflow can be used to commercially produce thousands of devices per day with minimal capital investment. Future work will demonstrate that other features of traditional microfluidics, including electrodes, valves, and sensors can also be integrated into PDMS or paper structure for µPiP-based electrochemical and electrokinetic analysis. We therefore expect that µPiP will be beneficial for both academia and industry, and serve as a powerful method to potentially bridge the translation and product develop gap between rapid device prototyping in academia and that of industrial scale microfluidic manufacturing, and serve as a low-cost minimal barrier of entry for researchers interested in micro fluidics.

**Figures**

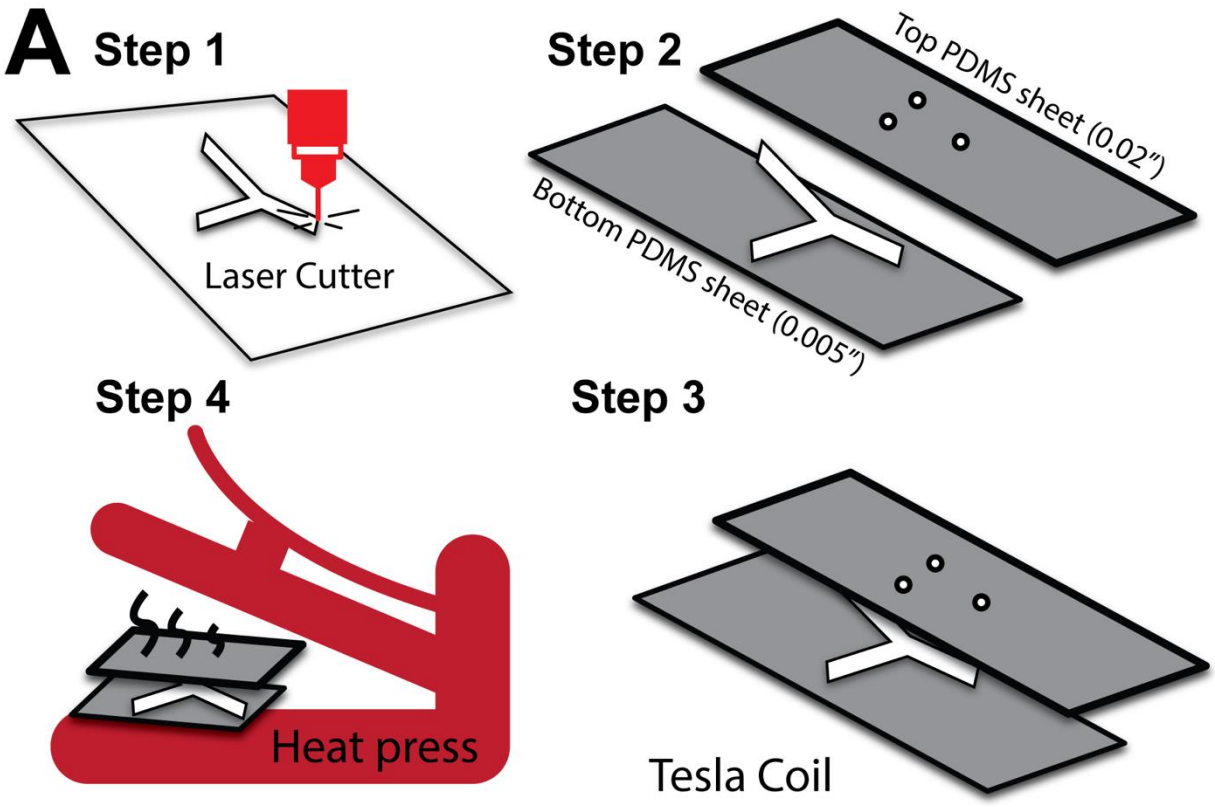


**Fig. 1.** Fabrication steps for “Microfluidic Pressure in Paper” (µPiP). Paper channels are patterned from a paper sheet using a $CO_2$ laser cutter. The channel is sandwiched between two thin sheets of PDMS. The PDMS sheets are corona treated with a Tesla coil and bonded together. Finally, the paper channels are conformally compressed and laminated using a hydraulic heat press.

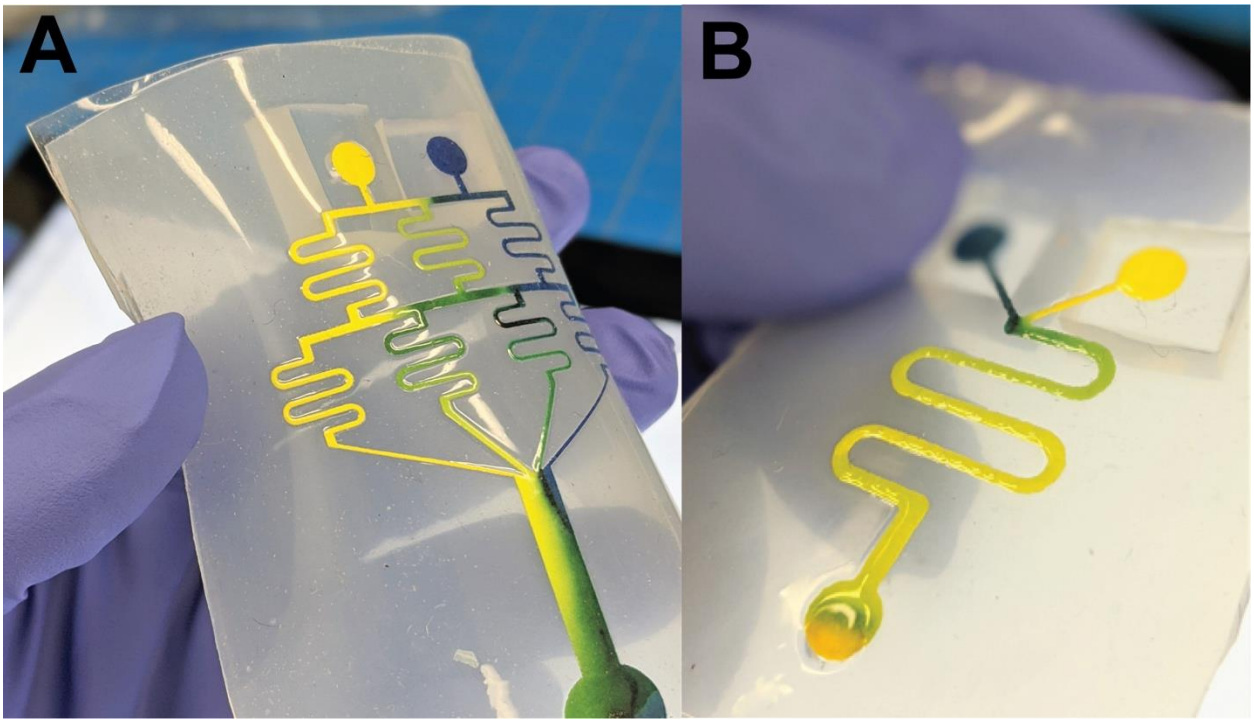


**Fig. 2** Fabricated µPiP devices are tightly laminated flexible fluidic structures capable of sustaining continuous pressure driven fluid flow. Two different devices are shown here after undergoing pressure driven flows. (b) A µPiP Gradient Generator. (b) A µPiP Serpentine Mixer.

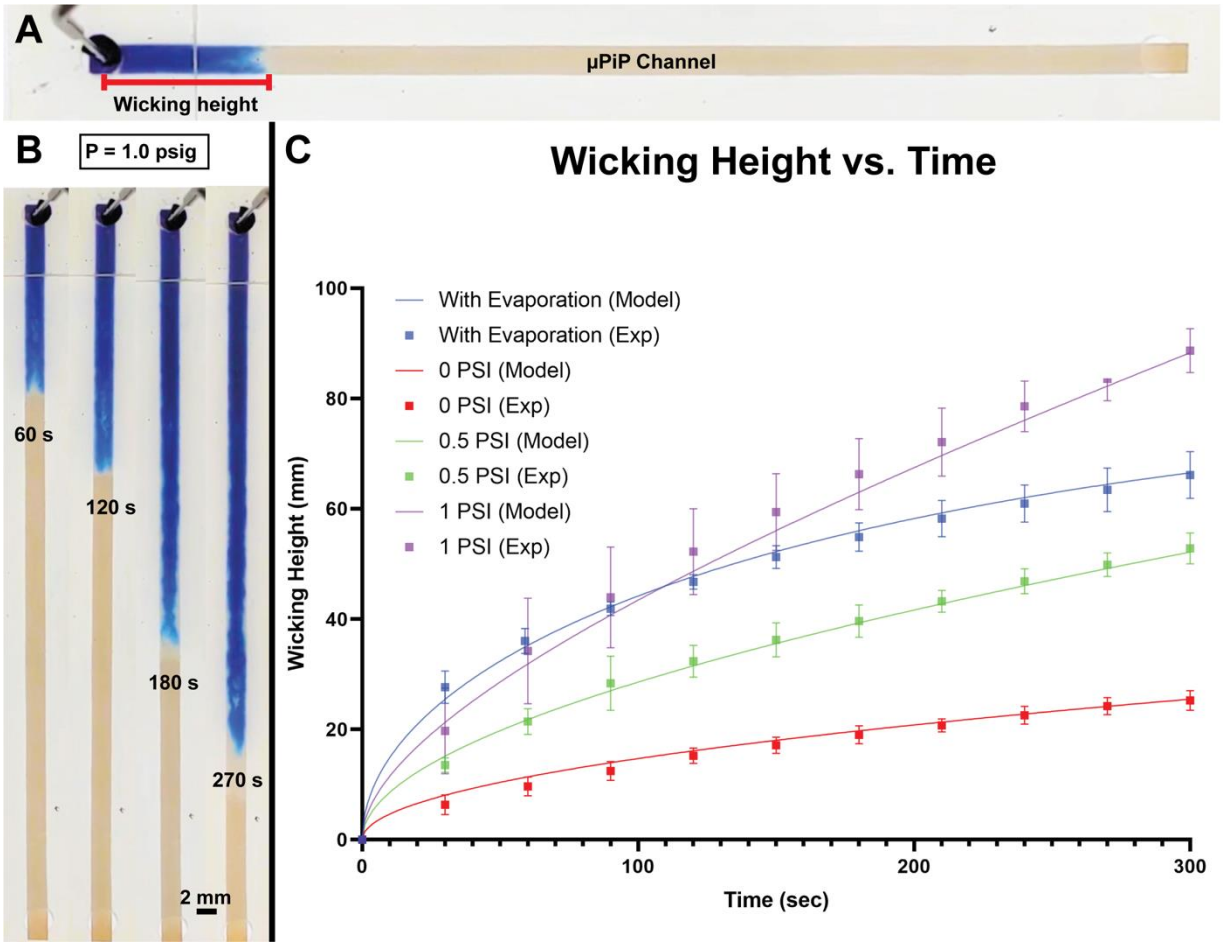


**Fig. 3** Experimental wicking height as a function of time down a μPiP channel. (a) Fluid flow observed as a penetrating wicking height. (b) Wicking height of colored deionized water in response to an external pressure at different time points. (c) Comparison of experimental wicking height with the mathematical model for capillary driven flow with evaporation (blue), capillary flow for compressed paper (red), capillary and pressure driven flow at different applied pressure (green and purple).

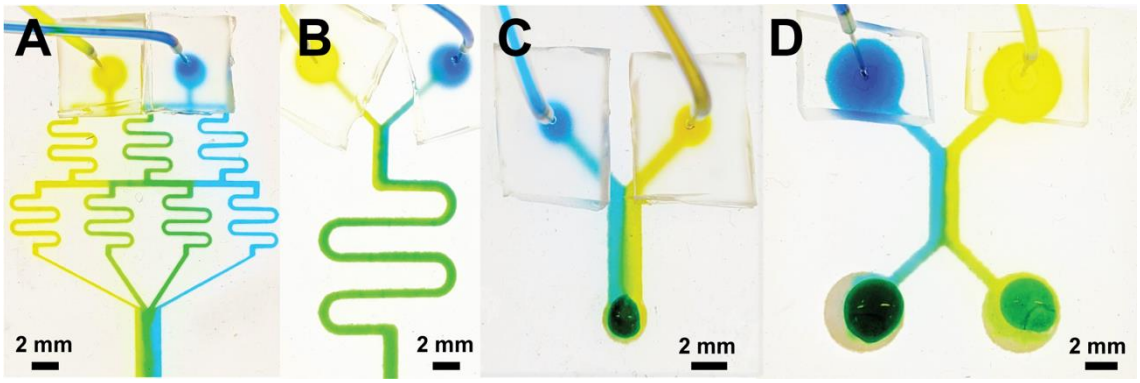


**Fig. 4** Common microfluidic geometries produced by the “Microfluidic Pressure in Paper” (µPiP) method. (a) Gradient generator. (b) Serpentine mixer. (c) Y-channel. (d) H-filter.

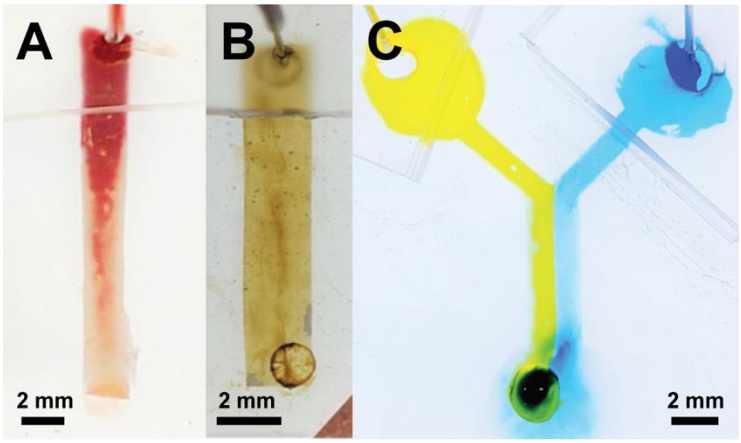


**Fig. 5** (a) Blood cell transport using µPiP. (b) Image of crude oil penetrating a µPiP channel. (b) Open and traditional style PDMS channel fabricated by µPiP with water soluble paper.

## References


1. Convery, N. and N. Gadegaard, *30 years of microfluidics.* Micro and Nano Engineering, 2019. **2**: p. 76-91.
2. Faustino, V., et al., *Biomedical microfluidic devices by using low-cost fabrication techniques: A review.* J Biomech, 2016. **49**(11): p. 2280-2292.
3. Walsh, D.I., 3rd, et al., *Enabling Microfluidics: from Clean Rooms to Makerspaces.* Trends Biotechnol, 2017. **35**(5): p. 383-392.
4. *Microfluidics Market Size, Share & Trends Analysis Report By Application (Lab-on-a-Chip, Organs-on-Chips, Continuous Flow), By Technology (Medical, Non-Medical), By Material, And Segment Forecasts, 2020 - 2027*. 2020, Grand View Research.
5. Gale, B., et al., *A Review of Current Methods in Microfluidic Device Fabrication and Future Commercialization Prospects.* Inventions, 2018. **3**(3).
6. Carrell, C., et al., *Beyond the lateral flow assay: A review of paper-based microfluidics.* Microelectronic Engineering, 2019. **206**: p. 45-54.
7. Martinez, A.W., et al., *Patterned paper as a platform for inexpensive, low-volume, portable bioassays.* Angew Chem Int Ed Engl, 2007. **46**(8): p. 1318-20.
8. Sher, M., et al., *Paper-based analytical devices for clinical diagnosis: recent advances in the fabrication techniques and sensing mechanisms.* Expert Rev Mol Diagn, 2017. **17**(4): p. 351-366.
9. Soum, V., et al., *Programmable Paper-Based Microfluidic Devices for Biomarker Detections.* Micromachines (Basel), 2019. **10**(8).
10. Osborn, J.L., et al., *Microfluidics without pumps: reinventing the T-sensor and H-filter in paper networks.* Lab Chip, 2010. **10**(20): p. 2659-65.
11. Määttänen, A., et al., *Paper-based planar reaction arrays for printed diagnostics.* Sensors and Actuators B: Chemical, 2011. **160**(1): p. 1404-1412.
12. Islam, M.N., et al., *Developing Paper Based Diagnostic Technique to Detect Uric Acid in Urine.* Front Chem, 2018. **6**: p. 496.
13. Andres W. Martinez, S.T.P., Emanuel Carrilho, and George M. Whitesides, *Diagnostics for the Developing World: Microfluidic Paper-Based Analytical Devices.* Analytical Chemistry, 2010(82): p. 3-10.
14. Cheng, C.M., et al., *Paper-based ELISA.* Angew Chem Int Ed Engl, 2010. **49**(28): p. 4771-4.
15. Jokerst, J.C., et al., *Development of a paper-based analytical device for colorimetric detection of select foodborne pathogens.* Anal Chem, 2012. **84**(6): p. 2900-7.
16. Mavrogiannis, N., et al., *Microfluidics made easy: A robust low-cost constant pressure flow controller for engineers and cell biologists.* Biomicrofluidics, 2016. **10**(3): p. 034107.
17. Cassano, C.L. and Z.H. Fan, *Laminated paper-based analytical devices (LPAD): fabrication, characterization, and assays.* Microfluidics and Nanofluidics, 2013. **15**(2): p. 173-181.
18. Channon, R.B., et al., *Rapid flow in multilayer microfluidic paper-based analytical devices.* Lab Chip, 2018. **18**(5): p. 793-802.

19. Liu, Z., et al., *Experimental and numerical studies on liquid wicking into filter papers for paper-based diagnostics.* Applied Thermal Engineering, 2015. **88**: p. 280-287.
20. MacDonald, B.D., *Flow of liquids through paper.* Journal of Fluid Mechanics, 2018. **852**: p. 1-4.
21. Mai, V.-P., C.-H. Ku, and R.-J. Yang, *Porosity estimation using electric current measurements for paper-based microfluidics.* Microfluidics and Nanofluidics, 2019. **23**(4).
22. *Plasma separation media*. 2017, Ahlstrom-Munksjö CytoSep®.
23. van den Tillaart, S.A., M.P. Busard, and J.B. Trimbos, *The use of distilled water in the achievement of local hemostasis during surgery.* Gynecol Surg, 2009. **6**(3): p. 255-259.